Six-dimensional Fourier analysis of the icosahedral $Al_{73}Mn_{21}Si_6$ alloy

D. Gratias
Centre d'Etudes de Chemie Metallurgique, Centre National de la Recherche Scientifique, 15 rue Georges Urbain, 94407 Vitry, France

J. W. Cahn and B. Mozer
Institute for Materials Science and Engineering, National Bureau of Standards, Gaithersburg, Maryland 20899
(Received 3 February 1988)

Fourier analysis of x-ray and neutron diffraction data of an icosahedral alloy are displayed both as a three-dimensional (3D) quasiperiodic function and as a six-dimensional (6D) periodic function. The 6D analysis leads to a simpler description that contains the same information as the 3D analysis. The 6D function has only two elongated peaks in the unit cell, but each peak contains much chemical detail.

In the preceding paper[1] we presented a Patterson analysis of an (Al,Si)-Mn icosahedral quasicrystal using x-ray and neutron diffraction data obtained from powders and compared it with an equivalent analysis done on the periodic crystalline α phase of the same elements. This Patterson analysis yields a quasiperiodic three-dimensional (3D) function describing the interatomic distance vectors. Because all diffraction vectors can be described in terms of six basis vectors,[2-6] this function can always be represented as a cut of a periodic 6D Patterson function (PF).[7,8] In this letter we construct this 6D function from the data and show that it is in many ways a simpler way of representing the distance vectors in the structure. The procedure is a simple extension of the technique used for incommensurate structures.[9]

The basis of the 3D PF is chosen as unit vectors along the six five-fold axes, and the indexing of the powder pattern assigns each peak to one (and occasionally more than one) icosahedral orbit expressed in terms of this basis.[1,6] As a result each 3D $\mathbf{k}$ vector can be represented as a 6D vector $\mathbf{K}$ on a primitive lattice (a $\mathbb{Z}^6$ module), and we define a 6D PF ($\mathbf{R}\in\mathbb{R}^6$) by

$$P(\mathbf{R})=\sum_{\mathbf{K}} I(\mathbf{K})e^{2i\pi\mathbf{K}\cdot\mathbf{R}} . \tag{1}$$

The 3D PF is recovered by a 3D cut on a plane defined by three equations $\mathbf{R}\cdot\mathbf{E}_\perp=0$, where $\mathbf{E}_\perp$ are three irrational vectors that define the space perpendicular to the icosahedral cut. Decomposing the 6D vectors $\mathbf{R}$ and $\mathbf{K}$ into components perpendicular and parallel to the cut plane,

$$\mathbf{R}=\mathbf{r}_\parallel+\mathbf{r}_\perp,\quad \mathbf{K}=\mathbf{k}_\parallel+\mathbf{k}_\perp , \tag{2}$$

and identifying $I(\mathbf{K})$ with $I(\mathbf{k}_\parallel)$ demonstrates that

$$P(\mathbf{R}=\mathbf{r}_\parallel)=\sum_{\mathbf{k}_\parallel} I(\mathbf{k}_\parallel)e^{2i\pi\mathbf{k}_\parallel\cdot\mathbf{r}_\parallel} \tag{3}$$

is identical to the definition of the 3D PF of our preceding paper.[1]

The Fourier transforms were carried out with the data[10,11] in Table I. The 6*D* x-ray PF shows only two peaks per unit cell; one centered on the origin, the other on the body center.[12] Both are elongated almost spherically in the perpendicular space. These aspects of the 6D PF's are best displayed on rational (to preserve the periodicity) 2D planes. Figure 1 shows two such planes, each of which was chosen to intercept real space along a symmetry axis of the icosahedral group: the plane $(xyyyy\bar{y})$ contains a fivefold axis, and the plane $(xxy0y0)$ contains a twofold one. The notation implies four equations that define these planes, e.g., $x_1=x_2$, $x_3=x_5$, and $x_4=x_6=0$ for the twofold plane. The figure clearly exhibits periodically arrayed ellipsoids. The nodal peak is elongated in the perpendicular space by almost the same extent in these two different views. The fivefold plane goes through the body center.

All peaks of the 3D PF seem solely to result from the intersection of the cut plane with these two peaks. This is illustrated in Figs. 1(a) and 2. In Fig. 1(a), we show a sector of the twofold plane of real space, which contains the twofold and fivefold axes, and compare this with the rational planes containing the same axes. We see at once that one unit cell of these rational planes contains the quasiperiodic PF to infinity along these symmetry axes. When the traces parallel to real space cross the unit-cell edge, its continuation in the next cell is identical to a parallel one in the original cell. Hence, 2D plots such as Figs. 1(b) and 1(c) may be seen as an infinite folding of a 1D function in physical space. Similarly, the 6D unit cell is such a folding of the 3D quasiperiodic function, which eventually samples every part of the unit cell.

Figure 2 shows the projections of all nodes and body centers of the 6D lattice onto the twofold plane of physical space with circle sizes indicating the proximity of the 6D point to physical space. A comparison of Fig. 2 with the corresponding parts of the 3D PF's [see Fig. 1(a) and our preceding paper] show that all peaks on the twofold plane result from just these two peaks in six dimensions. Except for the minor shifts, all interatomic distance vectors are thus determined. We may distinguish two kinds of translations: quasilattice translations associated with

 ©1988 The American Physical Society

TABLE I. Experimental integrated intensities for neutron (Ref. 10) absolute x-ray (Ref. 11) powder diffraction of $Al_{73}Mn_{21}Si_6$ icosahedral phase. Diffraction vectors $\mathbf{q}$ are at $(h+h'\tau, k+k'\tau, l+l'\tau)/[2(2+\tau)]^{1/2}A$ in 3D reciprocal space and the magnitude of q, $|\mathbf{q}| = A^{-1}[(N+M\tau)/2(2+\tau)]^{1/2}$, as obtained from powder diffraction angles, is parametrized by N and M.

		R^3 coordinates	Multi-	Intensity				R^3 coordinates	Multi-	Intensity	
N	M	hh' kk' ll'	plicity	Neutron	x-ray	N	M	hh' kk' ll'	plicity	Neutron	x-ray
0	0	00 00 00	1	0.00	1.0013	38	61	34 23 00	60	41.60	0.4997
2	1	10 01 00	12	1.88	0.00	40	64	24 24 00	60	20.70	0.0966
4	4	02 00 00	30	0.00	0.0017	46	73	12 45 00	60	99.60	0.0220
6	5	10 21 00	60	1.48	0.00	46	73	36 01 00	60	99.60	0.0220
6	9	12 01 00	20	72.90	0.1215	48	76	35 23 10	120	107.80	0.0870
8	12	22 00 00	30	44.90	0.0315	52	80	24 44 00	60	16.00	0.00
12	16	02 22 00	12	2.26	0.0011	52	80	44 24 00	60	16.00	0.00
12	16	22 02 00	60	11.30	0.0054	52	84	46 00 00	30	251.00	1.9189
14	17	32 01 00	60	11.80	0.0040	56	88	02 46 00	60	0.00	0.0167
14	17	12 03 00	60	11.80	0.0040	56	88	46 02 00	60	0.00	0.0167
14	21	10 23 00	60	129.00	0.0520	58	93	36 23 00	60	255.00	0.0502
16	24	22 22 00	60	131.00	0.00	60	96	46 22 00	20	36.00	0.0163
18	25	14 01 00	60	24.00	0.00	60	96	22 46 00	60	107.90	0.0488
18	29	12 23 00	12	1.82	1.2210	66	105	10 47 00	60	0.00	0.0427
20	28	33 01 10	120	28.00	0.00	66	105	34 45 00	60	0.00	0.0427
20	32	24 00 00	30	66.00	2.0896	70	113	12 47 00	60	0.00	0.6856
24	36	02 24 00	60	13.00	0.00	72	116	24 46 00	12	0.00	0.0837
24	36	24 02 00	20	4.00	0.00	72	116	46 24 00	60	0.00	0.4184
26	41	34 01 00	60	51.00	0.00	78	125	46 34 01	120	141.50	0.00
28	44	24 22 00	60	55.00	0.0819	80	128	48 00 00	30	20.10	0.00
28	44	22 24 00	12	11.00	0.0164	80	128	12 57 01	120	80.40	0.00
30	45	14 23 00	60	24.20	0.00	86	137	36 45 00	60	38.20	0.00
30	45	34 21 00	20	8.10	0.00	86	137	47 24 10	120	76.40	0.00
30	45	10 25 00	60	24.20	0.00	98	157	22 58 01	120	347.00	0.00
32	48	11 25 10	120	6.30	0.0062	110	177	59 11 11	120	221.00	0.00
32	48	44 00 00	30	1.60	0.0015	110	177	36 47 00	60	111.00	0.00
34	49	01 44 10	120	0.00	0.0030	118	189	47 46 10	120	71.80	0.00
34	49	34 03 00	60	0.00	0.0015	118	189	58 25 00	60	35.90	0.00
34	53	12 25 00	60	98.50	0.0226	118	189	10 69 00	60	35.90	0.00

the nodal peak (solid circles), and those associated with the body-centered peak (dashed circles), which we will term motif translations.

Structural information is also contained in the magnitudes of these peaks and their shifts from their ideal position. This is examined next again in six dimensions and compared with our neutron results.

Neutron data are especially useful because of the negative scattering length of manganese. Heteroatomic distances contribute negatively to the neutron PF. Figure 3 shows our neutron results for the same planes as in Figs. 1(b) and 1(c). The same two peaks appear, but they change sign as the perpendicular distance increases. The body center is now negative. The same result is shown in Fig. 4, where we show the magnitude of the 3D PF at the exact projected positions (as in Fig. 2, but all in real space) as a function of the magnitude of $\mathbf{r}_\perp$. The spread in these curves is due to deviations from spherical symmetry of the 6D peaks in $\mathbb{E}_\perp$. These results indicate that the two peaks in the 6D pattern have an internal structure that reflect the chemical ordering in the quasicrystal.

In a periodic crystal, a lattice translation superimposes the crystal upon itself. A good quasilattice translation, defined as one with a small $\mathbf{r}_\perp$, can be seen in the PF, Fig. 4, to have a Patterson peak that is large in both x rays and neutrons. It indicates that a large fraction of the quasicrystal is superimposed upon itself after the real-space translation, with like atoms on top of each other. As the value of $\mathbf{r}_\perp$ increases, not only is there less superpositioning of atoms, but increasingly the superimposed atoms differ chemically. This shows that atom-packing geometries result in longer-range quasilattice translations than would be obtained by chemical correlations.

In a periodic crystal, all interatomic distance vectors that are not lattice translations define motif translations. The α-(Al,Si)Mn structure with 138 atoms per unit cell on 11 orbits has many motif translations and a quite complicated PF, but each motif translation is definitely either homoatomic or heteroatomic. In the quasicrystal, many of these distances are slightly shifted and become identified with only two 6D peaks, but each 6D peak contains a spectrum of chemical character that depends primarily on the magnitude of $\mathbf{r}_\perp$. The good quasicrystalline motif translations (with small $\mathbf{r}_\perp$) are primarily heteroa-

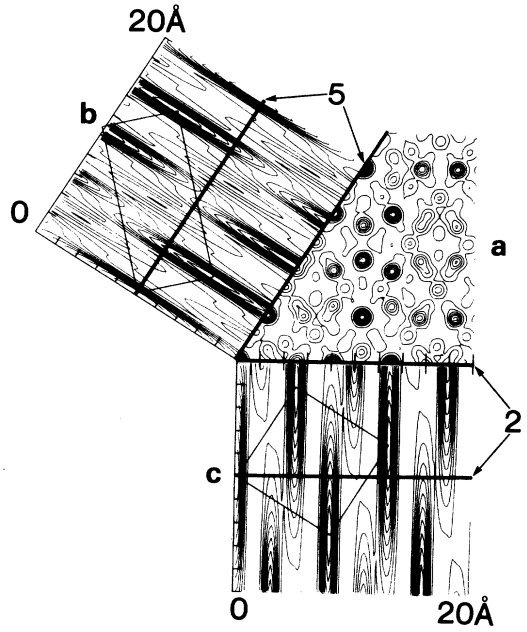

FIG. 1. (a) The twofold plane of the real-space x-ray PF, together with two views of the 6D x-ray PF along rational planes each aligned to have its real-space axis parallel to the corresponding axis of (a) containing a real-space axis; (b) $(xyyyy\bar{y})$ containing the body center of the 6D cell and the five-fold axis; (c) $(xxy0y0)$ containing the twofold axis, as well as some saddles at special points of the unit cell. The rectangular grids in (b) and (c) outline the cell boundaries. The quasiperiodic arrangement of peaks in real space is seen as following the arrangement of peaks along an irrational direction in the 6D PF. Contours go from 0 to 1 in steps of 0.1.

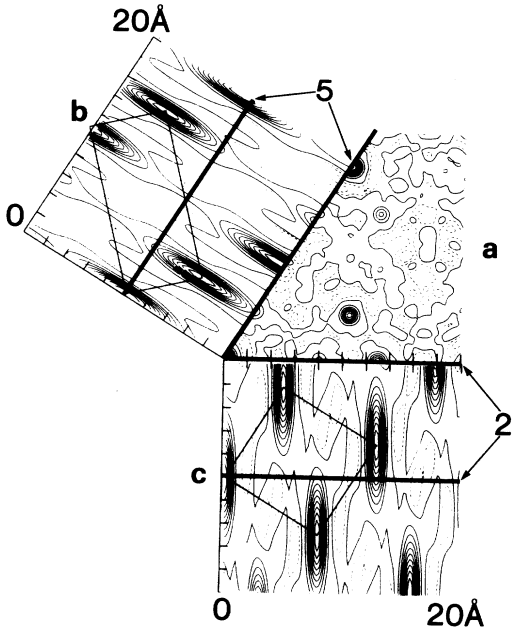

FIG. 3. The neutron PF for the same planes as in Fig. 1, showing that the peaks change sign with perpendicular distance from their center, indicating changes in the chemical nature of the peaks. Negative contours are dashed and separated by 0.03 and positive contours go from 0 to 1 in steps of 0.1.

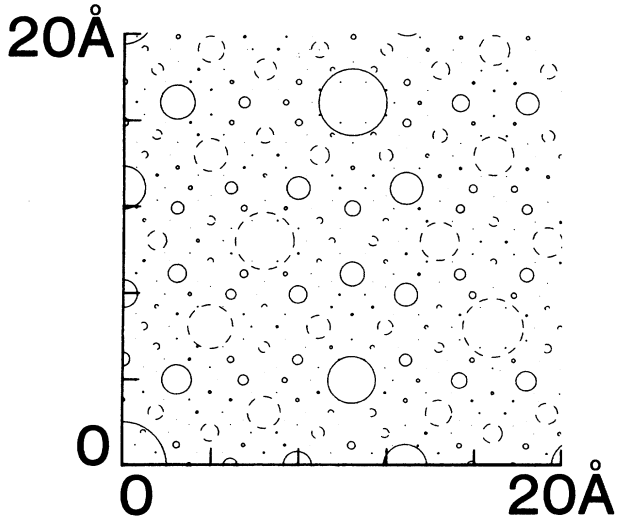

FIG. 2. The projection of all nearby 6D nodes and body centers onto the twofold real-space plane. Comparison with the x-ray PF for this plane [Fig. 1(a) of Ref. 1] shows that all peaks originate from these 6D points. Solid circles are nodes and dashed circles are body centers.

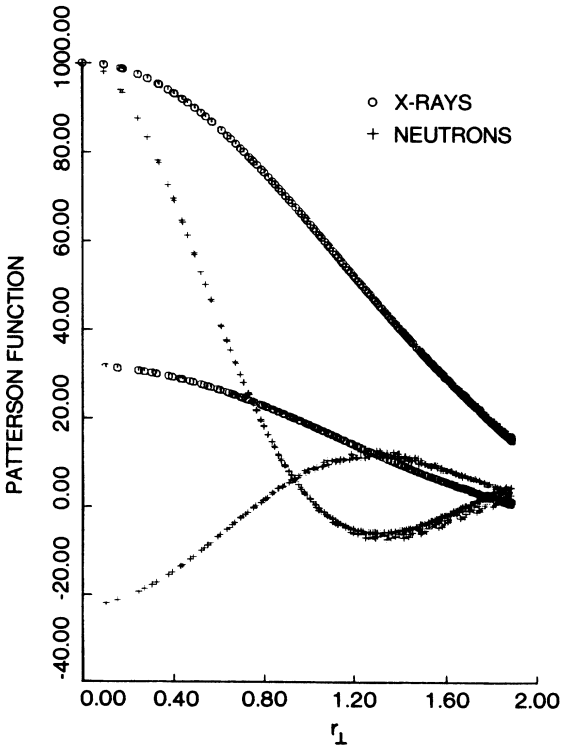

FIG. 4. The x-ray and neutron Patterson intensities at real-space projections of 6D nodes and body centers as a function of the magnitude of $\mathbf{r}_\perp$. The difference between x rays and neutrons indicates the degree of heteroatomic character for the corresponding real-space distances.

tomic distance.

The slight shifts in the peak positions of the 3D PF can now be seen as resulting from chemical and steric effects. Al is larger than Mn, and the homoatomic distances are dominated by the most common atom. The heteroatomic distances are slightly smaller. A comparison between the 6D x-ray and neutron peaks shows that as $\mathbf{r}_\perp$ increases chemical differences arise across the peak in the $\mathbf{r}_\parallel$ direction. As a result, the peaks in 3D space will be seen as multiple peaks, with the neutron results identifying which ones are homoatomic or heteroatomic. Similarly, there are steric effects. Where real space skirts the outer edges of a 6D peak, there is less likelihood of an interatomic distance. The chemical nature of both the atoms at this and those at nearby distances is affected by the increasing likelihood of vacant space. At the outer fringes of a peak, other peaks curve to fill the empty space, or, in other views of the 6D space, curve to join and thereby continue a peak. In these regions, comparison of neutron with x-ray results show strong chemical effects.

The discovery of quasicrystals has raised many problems for crystallographers. One of these is how to describe their structure. We have examined with the empirical Patterson analysis two of the possibilities: a real-space 3D aperiodic function and a periodic 6D function. All we could say about the 3D analysis was that the result was complicated, but that it proved to be quite similar at short distances to the α crystal and that patterns repeated over and over again, but never quite in exactly the same way. We find that this 3D complexity has a simpler two-peak description in six dimensions with structural information contained in the details of the peaks. The 6D PF of the quasicrystal is in many ways simpler even than that of the 3D α periodic structure.

Note added in proof. Since these papers were submitted, we have constructed a 6D model of the structure of this alloy, based on the results of this and the preceding paper.[1] The known atomic positions in the 11 orbits of the α crystal are used to determine positions of five 6D orbits. Intensities calculated from the model, with a static Debye-Waller as the only fitting parameter, fit the x-ray intensities with an R of 0.13. An article will appear in J. Phys. (Paris) **49**, No. 7 (1988).

[1]J. W. Cahn, D. Gratias, and B. Mozer, preceding paper, Phys. Rev. B **38**, 1638 (1988).

[2]V. Elser, Acta Crystallogr. Sect. A **42**, 36 (1985); Phys. Rev. Lett. **55**, 2883 (1985); Phys. Rev. B **32**, 4892 (1985).

[3]M. Duneau and A. Katz, Phys. Rev. Lett. **54**, 2688 (1985); A. Katz and M. Duneau, J. Phys. (Paris) **47**, 181 (1986); J. Phys. (Paris) Colloq. **47**, C3-103 (1986).

[4]F. Gahler and J. Rhyner, Phys. Rev. Lett. **55**, 2369 (1985); J. Phys. A **19**, 267 (1985).

[5]P. Bak, Phys. Rev. Lett. **54**, 1517 (1985); Phys. Rev. B **32**, 5764 (1985); Phys. Rev. Lett. **56**, 861 (1986).

[6]J. W. Cahn, D. Gratias, and D. Shechtman, J. Mater. Res. **1**, 13 (1986).

[7]H. Bohr, Acta Math. **45**, 29 (1924); **46**, 101 (1925); **47**, 237 (1926).

[8]A. S. Besicovitch, *Almost Periodic Functions* (Cambridge University, Cambridge, 1932).

[9]W. Steurer, Acta Crystallogr. Sect. A **43**, 36 (1987), and references therein.

[10]R. Bellissent, J. W. Cahn, D. Gratias, B. Mozer, and J. L. Soubeyrous (unpublished).

[11]D. Gratias, J. W. Cahn, M. Bessiere, Y. Calvayrac, S. Lefebvre, A. Quivy, and B. Mozer, in *New Concepts in Physical Chemistry,* Proceedings of the NATO Advanced Research Workshop, Aqua-Freda, 1987 (unpublished).

[12]We expected the oscillations inherent in such truncated Fourier analysis to lead to many artifactual maxima. In six dimensions, saddles abounded, but we found only two peaks.